# A low-cost microwell device for high-resolution imaging of neurite outgrowth in 3D

**Yuan Ren[1], Michael J Mlodzianoski[2], Aih Cheun Lee[1], Fang Huang[2,3,4]** (iD)
**and Daniel M Suter[1,4,5,6,7]** (iD)

[1] Department of Biological Sciences, Purdue University, West Lafayette, IN 47907, United States of America
[2] Weldon School of Biomedical Engineering, Purdue University, West Lafayette, IN 47907,
United States of America
[3] Purdue Institute of Inflammation, Immunology and Infectious Disease, Purdue University,
West Lafayette, IN, United States of America
[4] Purdue Institute for Integrative Neuroscience, Purdue University, West Lafayette, IN 47907,
United States of America
[5] Bindley Bioscience Center, Purdue University, West Lafayette, IN 47907, United States of America
[6] Birck Nanotechnology Center, Purdue University, West Lafayette, IN 47907, United States of America

E-mail: dsuter@purdue.edu

CrossMark

## Abstract

*Objective.* Current neuronal cell culture is mostly performed on two-dimensional (2D) surfaces, which lack many of the important features of the native environment of neurons, including topographical cues, deformable extracellular matrix, and spatial isotropy or anisotropy in three dimensions. Although three-dimensional (3D) cell culture systems provide a more physiologically relevant environment than 2D systems, their popularity is greatly hampered by the lack of easy-to-make-and-use devices. We aim to develop a widely applicable 3D culture procedure to facilitate the transition of neuronal cultures from 2D to 3D. *Approach.* We made a simple microwell device for 3D neuronal cell culture that is inexpensive, easy to assemble, and fully compatible with commonly used imaging techniques, including super-resolution microscopy. *Main results.* We developed a novel gel mixture to support 3D neurite regeneration of *Aplysia* bag cell neurons, a system that has been extensively used for quantitative analysis of growth cone dynamics in 2D. We found that the morphology and growth pattern of bag cell growth cones in 3D culture closely resemble the ones of growth cones observed *in vivo*. We demonstrated the capability of our device for high-resolution imaging of cytoskeletal and signaling proteins as well as organelles. *Significance.* Neuronal cell culture has been a valuable tool for neuroscientists to study the behavior of neurons in a controlled environment. Compared to 2D, neurons cultured in 3D retain the majority of their native characteristics, while offering higher accessibility, control, and repeatability. We expect that our microwell device will facilitate a wider adoption of 3D neuronal cultures to study the mechanisms of neurite regeneration.

Keywords: 3D culture, neuron, neurite outgrowth, high resolution imaging, growth cone, cytoskeleton, cell culture

S Supplementary material for this article is available online

(Some figures may appear in colour only in the online journal)

---

[7] Author to whom any correspondence should be addressed.
Department of Biological Sciences, Purdue University, 915 West State Street, West Lafayette, IN 47907-2054, United States of America.

# 1. Introduction

Axonal growth and guidance are critical processes during both development and regeneration of the nervous system. They can be studied *in vivo* either in normal or perturbed physiological environments [1, 2]. In recent years, *in vivo* studies have benefited from rapid developments of breakthrough technologies such as deep tissue live imaging [3–5], tissue clearing [6, 7], and genome editing [8, 9]. Whereas *in vivo* approaches have the benefit that neurons develop axons and dendrites in a physiological environment, they suffer from the lack of complete control of the environment. This advantage is present when neurons are cultured *in vitro* in an experimentally defined environment that is permissive for neurite regeneration [10–12]. However, the potential of such *in vitro* studies is increasingly impeded by the limitations of the traditionally used cell culture method, namely two-dimensional (2D) culture. In its most common form, 2D culture involves plating of cells on flat and rigid surfaces with protein coatings of varying degrees of biological relevance. Drastically different from three-dimensional (3D) *in vivo* environments, the 2D culture method forces all cellular activities to be carried out on a flat surface of non-physiological stiffness, which induces a strong polarization orthogonal to the plane while missing key features such as topographical cues and proper interaction with the extracellular matrix (ECM) [13–15]. This imposes additional challenges to cultured neurons because of the restraints on growth and guidance of developing neurites for inter-neuronal wiring [16–18]. Although neurite regeneration can happen on 2D substrates, neurons cultured as such have been shown to have substantially altered morphology [18–20], excitability [21, 22], and gene expression profile [19, 23], which may not only confound data interpretation, but also severely diminish the translational power of experimental results [24].

To bridge the gap between *in vivo* and *in vitro* studies, a number of devices and biocompatible materials have been developed for 3D neuronal cell cultures, which better mimic the native environment of cells while offering freedom of experimental control [20, 25–27]. Natural polymers such as collagen gels [21, 28–31], artificially synthesized scaffolds [13, 22, 32, 33], and artificial hydrogels [20, 34, 35] are on the growing list of 3D culture methods, each tailored to specific needs of the research community. However, despite the clear caveats of 2D culture systems and numerous avenues opened up by 3D culture techniques, the former approach has remained more popular in current bioscience research. We believe that this is largely because many published 3D culture devices and materials require special instruments to fabricate them (3D-printer, electrospinning machine, photo or chemical etching instrument) and because many available protocols are either expensive or challenging to follow, or have only narrow applications. As a result, a typical lab would have to rely on 2D culture for *in vitro* research, viewing 3D culture only as an auxiliary or supplementary approach. A versatile 3D neuronal culture microwell device, which is inexpensive and easy to make, would help erase the concerns about 3D culture-based procedures and accelerate the dissemination of biologically relevant knowledge.

In this paper, we demonstrate a novel microwell system for 3D neuronal cell cultures that is simple and inexpensive. We exemplify the utility of our device by culturing *Aplysia* bag cell neurons, a neuronal cell type commonly used for the study of peptide release, neuronal excitability, and growth cone dynamics [36, 37], for the first time in 3D using a novel collagen-based gel to induce neurite regeneration. We show the compatibility of our microwell with different modes of high-resolution imaging techniques for both fixed and live neurons, including differential interference contrast (DIC) microscopy, wide-field fluorescence, and super-resolution imaging of subcellular components. We believe that the affordability and simplicity of our device will make it a valuable addition to the arsenal of 3D culture systems, which will be of significant interest to the neuroscience community.

# 2. Materials and methods

## 2.1. Microwell fabrication

Plastic squares were cut from single sheet polyester shims (0.020 inch thickness, Yellow, SHSP-200, Small Parts, Inc., Miami Lakes, FL) as shown in figures 1(A)–(C). Before assembling the microwell, one side of the plastic square was covered with double-sided tape (3M 442KW double-sided film tape, S-18740, Uline, Pleasant Prairie, WI). Then, the yellow plastic piece was punched with quarter-inch hole puncher. A glass coverslip was attached to the plastic shim via the double-sided tape to make a tight seal (High performance cover glass, 0.17 mm thickness, 22 × 22 mm, 474030-9020-000, Carl Zeiss Microscopy, Thornwood, NY). We used high vacuum grease (High vacuum grease, 1018817, Dow Corning, Midland, MI) to adhere the microwell to the bottom of a 35 mm cell culture dish, so that the microwell does not fall when flipped during the gelling period (figure 1(D)). Next, the gel/cell mixture was added into the microwell, and the gel was allowed to solidify in the inverted Petri dish in a humidified 37 °C incubator for 50 min. After the gel had solidified, the dish was flipped around again in order to add L15 cell culture media (Thermo Fisher Scientific, Waltham, MA) supplemented with artificial seawater (ASW; 400 mM NaCl, 9 mM $CaCl_2$, 27 mM $MgSO_4$, 28 mM $MgCl_2$) [37, 38]. Petri dishes were kept at room temperature (RT) for 1–4 d. For low magnification imaging with a 10× long-working distance objective, neurons were directly imaged within the culture dish. For high magnification imaging, an imaging chamber was assembled with a second cover glass following a similar procedure as previously reported [37, 38] and as shown in figure 1(D). After imaging, the second cover glass was removed, and the microwell with neurons was put back into the culture dish with medium for continued growth.

## 2.2. Collagen gel mixture

The following collagen gel mixture was prepared: 50% volume of type I rat tail collagen (354236, Corning incorporated, Corning, NY), 15% volume of 5× ASW, 25% volume of *Aplysia* hemolymph, 10% volume of 200 $\mu g$ $ml^{-1}$
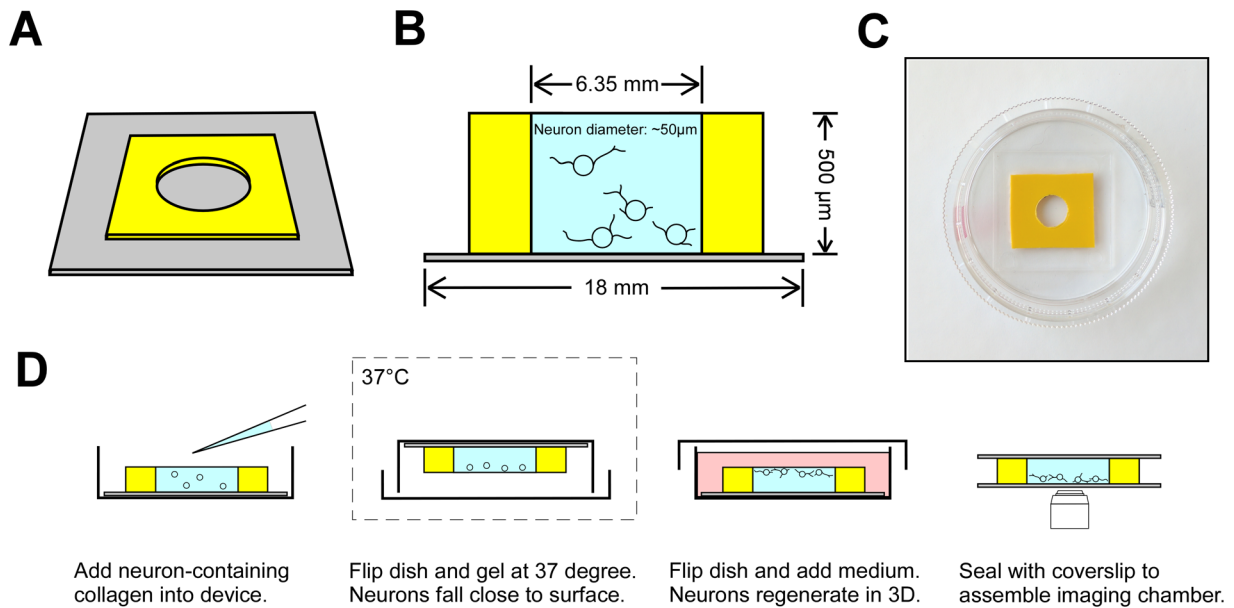
**Figure 1.** Design of 3D culture device. (A) Schematic showing top view of the microwell device mounted on a coverslip. (B) Side view of microwell filled with neuron-containing collagen gel. The height is exaggerated in this drawing for illustrative purpose. (C) Picture of a glass coverslip with an attached microwell in an empty Petri dish. (D) Schematic demonstrating the work flow of neuronal culture and imaging using the 3D culture device. A color version of this figure is available online.

poly-L-Lysine (PLL; poly-L-lysine hydrobromide, molecular weight 70 000–150 000, P6282, Sigma, St. Louis, MO), pH 7.9, osmolarity: 1000 mOsm. The final concentration of collagen was between 2–3 mg ml$^{-1}$. During the gel optimization process, four final concentrations of PLL (0 $\mu$g ml$^{-1}$, 10 $\mu$g ml$^{-1}$, 20 $\mu$g ml$^{-1}$, 40 $\mu$g ml$^{-1}$) and three concentrations of Hemolymph (0%, 10%, 25%) were compared. PLL was found to be critical for providing the collagen gel with the necessary mechanical strength in high-salt media. 20 $\mu$g ml$^{-1}$ PLL in the final gel mixture was the minimum to maintain a solid gel in cell culture medium, while no difference in the percentage of regenerating neurons was found between gels with PLL concentration 20 $\mu$g ml$^{-1}$ and 40 $\mu$g ml$^{-1}$. 25% hemolymph was the minimum amount required to induce robust neurite regeneration.

## 2.3. Neuronal cell culture

*Aplysia* bag cell neurons were obtained after enzymatic digestion of the abdominal ganglion from adult *Aplysia californica* (150–200 g, Marinus Scientific, Long Beach, CA) as previously reported [37, 38]. Typically 15–20 bag cell neurons were mixed with collagen gel solution described above and loaded into the microwell for culture. This low cell density was selected to avoid overlapping neurites from neighboring neurons, whereas regeneration of >50 *Aplysia* bag cell neurons in the same viewing plane can be supported simultaneously by our device. After the gel had solidified, L15-ASW was added as cell culture medium.

## 2.4. Fluorescent labeling

Neurons were fixed directly in the gel with 3.7% paraformaldehyde in ASW supplemented with 400 mM sucrose for

15 min before permeabilization was performed with 0.05% saponin in fixative solution for 10 min. The sample was then immersed in PBS/0.005% saponin for washing. Blocking was done with 5% bovine serum albumin (BSA) in phosphate-buffered saline (PBS) containing 0.005% saponin for 1 h. To stain microtubules, the primary antibody (mouse monoclonal anti-alpha-tubulin, clone B-5-1-2, Sigma) was diluted to 10 $\mu$g ml$^{-1}$ in blocking solution and incubated for 1 h. Following three washes with PBS/0.005% saponin, the secondary antibody (goat-anti-mouse Alexa-647, A-21235, Thermo Fisher Scientific) was diluted to 4 $\mu$g ml$^{-1}$ in PBS/0.005% saponin and incubated for 30 min. To stain F-actin, Alexa-488 Phalloidin (A12379, Thermo Scientific) was diluted to 66 nM in PBS/0.005% saponin and incubated for 30 min. After incubation with fluorescent probes, three washings with PBS/0.005% saponin were carried out before imaging. To label mitochondria in live neurons, TMRM (Tetramethylrhodamine, Methyl Ester, Perchlorate, T668, Thermo Fisher Scientific) was added to culture medium to a final concentration of 100 nM for 30 min before imaging. All labeling was done at RT.

## 2.5. mRNA preparation and injection

pRAT-Src1dSH2-EGFP is an *Aplysia*-specific biosensor for tyrosine phosphorylation and based on the YFP-dSH2 construct previously used in vertebrate cells [39]. To generate this construct, two SH2 domains derived from *Aplysia* Src1 were cloned in front of the N-terminus of EGFP in pRAT vector. The *Aplysia* Src1 SH2 domain sequence was used as a PCR template (Ap Src1 amino acids 126-224) flanked with 5′ PstI and 3′ AgeI restriction enzyme sites (forward primer: 5′ agctagctgcagatgacgccacagacgcaagactggt3′; reverse primer: 5′ agctagaccggtcccctggggcacgccgctcccag3′). A second round

of SH2 domain amplification generated a Src1 SH2 domain flanked with AgeI sites on both sides (forward primer: 5′ agctagaccggtaacgccacagacgcaagactggt 3′; reverse primer: 5′ agctagaccggtcccctggggcacgccgctcccag 3′). This SH2 domain was inserted into the AgeI site of pRAT-Src1SH2-EGFP to create pRAT-Src1dSH2-EGFP, the phosphotyrosine (pY) biosensor, which was verified with sequencing (Purdue Genomics Core Facility). mRNA of the pY sensor was made from the mMESSAGE mMACHINE T7 Ultra *in vitro* transcription kit (Ambion, Thermo Fisher Scientific) according to manufacturer's instruction. Typical mRNA concentration for injection was $0.5\,mg\,ml^{-1}$. mRNA was mixed with fluorescent dextran ($2.5\,mg\,ml^{-1}$ final concentration; 3 kD Texas red dextran, fixable, Thermo Fisher Scientific) before injection as previously reported [40]. Microinjection was performed in bag cell neurons embedded in gel using an NP2 micromanipulator and FemtoJet microinjection system (Eppendorf, Hauppauge, NY). Fluorescent protein expression was evaluated 24 h after microinjection.

### 2.6. Image acquisition and analysis

Except for super-resolution imaging, images were acquired on a Nikon TE2000 E2 inverted microscope (Nikon, Melville, NY) with $10\times$, $40\times$ air, $60\times$, or $100\times$ oil immersion objectives, sometimes with additional $1.5\times$ magnification. All imaging was performed at RT. Focus during extended time-lapse imaging was maintained by a Nikon Perfect Focus system. Fluorescent illumination was provided by an X-cite 120 metal halide lamp (EXFO, Quebec, QC, Canada) and appropriate filter sets (Chroma Technology, Bellows Falls, VT). Images were acquired by a Cascade II charge-coupled device (CCD) camera (Photometrics, Tucson, AZ) controlled with MetaMorph 7.8 software (Molecular Devices, Sunnyvale, CA). Image analysis was performed with either MetaMorph 7.8 or ImageJ software (available at https://imagej.nih.gov/ij/).

For super-resolution microscopy, raw data were recorded on a custom-built single molecule switching nanoscopy setup based around an Olympus IX-73 microscope stand (IX-73, Olympus America Inc., Waltham, MA) with a $100\times/1.35$ NA silicone oil-immersion objective lens (FV-U2B714, Olympus America Inc.), a 405 nm (DL-405-100, CrystaLaser, Reno, NV) for activation and a 642 nm laser (2RU-VFL-P-2000-642-B1R, MPB Communications Inc.) for excitation. The filter turret contained a quad bandpass (Di03-R405/488/561/635-t1 and FF01-446/523/600/677, Semrock Inc.). A Deformable Mirror (Multi-3.5, Boston Micromachines, Cambridge, MA) removed optical aberrations following the procedure described previously [41, 42]. Fluorescence passed through an additional bandpass filter (FF01-731/137-25, Semrock Inc.) placed just before the camera. The fluorescence signal was recorded on a sCMOS Orca-Flash4.0v3 (Hamamatsu, Tokyo, Japan). The overall system magnification was $\sim\!54\times$, resulting in an effective pixel size of 120 nm. Molecules were localized using previously described algorithms [42, 43].

## 3. Results

### 3.1. Device design and workflow

A simple device for 3D neuronal cell culture was developed by attaching a punched plastic chip to a standard #1.5 coverslip using waterproof double-sided tape (figure 1(A)). The cylindrical space created thereby has a volume of 16 $\mu$l and can be used as a chamber for 3D neuronal culture. To facilitate single cell neurite growth analysis, we have chosen bag cell neurons from *Aplysia californica*, which have a large cell soma, are easily identifiable *in vitro,* and have been used in a number of growth cone motility and neurite outgrowth studies [11, 36, 44]. As shown in figure 1(D), after the liquid gel mixture with neurons was loaded into the microwell and inverted during the gelling phase, gravitational force pulled neurons close to gel surface until further movement was balanced by the surface tension of the gel. This procedure typically positioned neurons within 50 $\mu$m of the gel surface, and this proximity was maintained after gel solidification, when the microwell was flipped again and medium added. Positioning of bag cell neuron is achieved within 5 min after inverting, but a typical gelling time of 50 min was chosen to ensure complete gel solidification. The distance between cell soma and gel surface is far enough to allow neurite regeneration in 3D with most regenerated neurites being close enough to the gel surface to be imaged with high-resolution objectives. In contrast to many current 3D culture methods, our setup eliminated the contact between soma and coverslip during cell culture, which has been shown to not only bias neurite outgrowth towards coverslip surface but also change gene expression patterns [19]. The short distance between neurons and culture media also makes it easy to apply cell-permeable molecules and inject cells as shown below. To induce neurite outgrowth, we created a novel collagen-based gel mixture, which contains 20 $\mu$g ml$^{-1}$ PLL and 25% *Aplysia* hemolymph. PLL helped to maintain the mechanical strength of collagen gel in high salt media, whereas hemolymph was found to be critical for stimulating neurite regeneration, possibly due to the presence of endogenous growth promoting factors. Both PLL and hemolymph were added at their minimum effective concentration to promote robust outgrowth at highest possible rates.

### 3.2. Neurite outgrowth in 3D

Bag cell neurons exhibited robust neurite regeneration in the 3D gel. As shown in figure 2(A), multiple neurites developed from the identified neuron between 24 and 30 h after neurons had been embedded (figure 2(A)). Contrary to the growth pattern on a coverslip, neurite outgrowth was no longer confined to a planar surface [18, 45]. The three-dimensional exploration of the gel space was evidenced by the neurite tips growing out of the plane of focus between 26 and 30 h (figure 2(A)). We could observe a variety of complex behaviors of neurite growth, including elongation, retraction, and branching (supplementary video 1 (stacks.iop.org/JNE/15/035001/mmedia)). In contrast
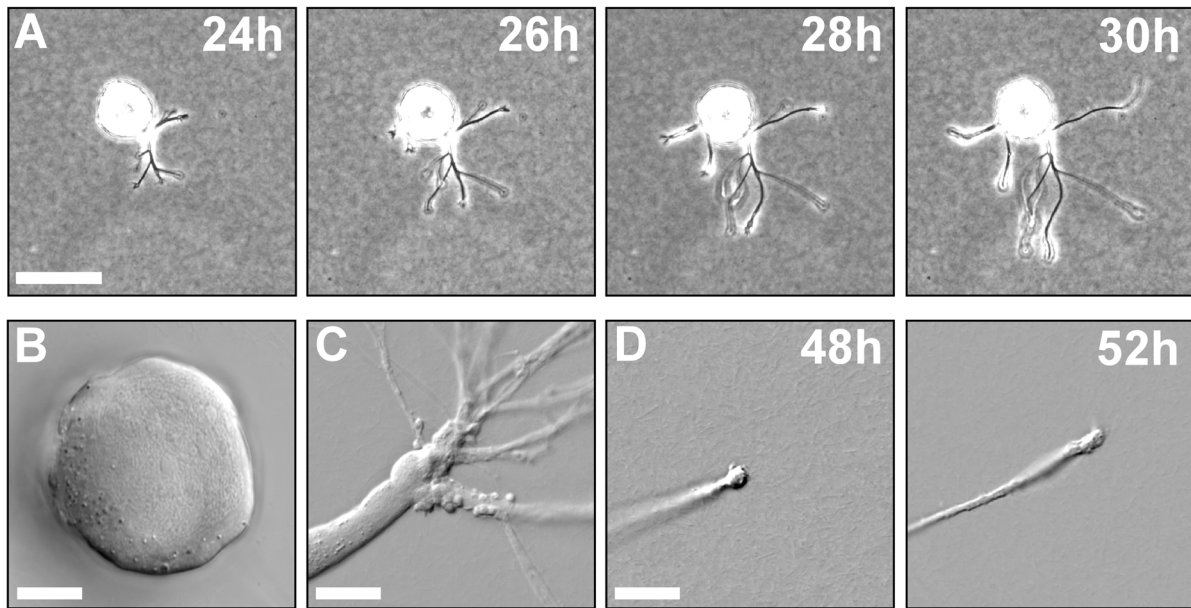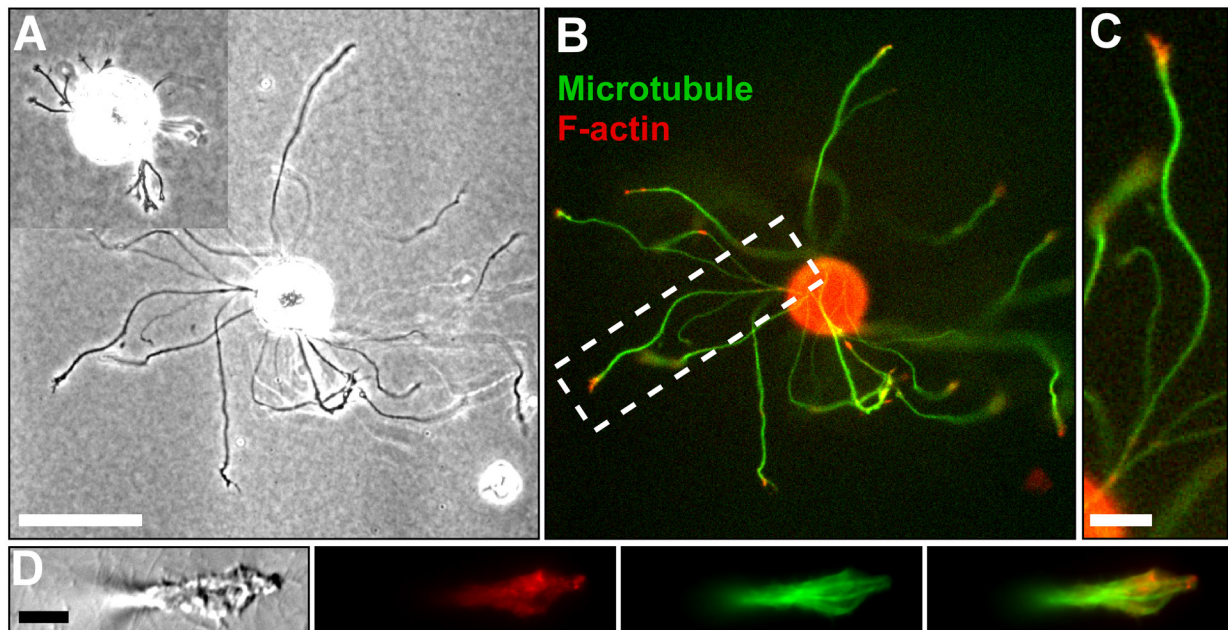
**Figure 2.** Neurite outgrowth in a 3D collagen gel. (A) Snapshots of a bag cell neuron regenerating neurites in 3D. Note the extension of neurites in multiple directions. See also supplementary video 1. (B) The cell body of a bag cell neuron in the gel retains spherical shape. (C) A neurite branching point with the mother neurite remaining in focus. Note the abundant daughter neurites growing in different directions. (D) A neuronal growth cone growing at an average rate of 5.2 $\mu$m h$^{-1}$ was imaged for 4 h. See also supplementary video 2. Scale bars: 50 $\mu$m (A); 20 $\mu$m (B)–(D).

to the flattened cell bodies commonly seen in 2D cultures [19, 23], the cell body of a bag cell neuron retained its spherical shape (figure 2(B)), again suggesting the isotropic property of the culture environment. The growth in 3D was very clear when a neurite branching point was imaged, where almost all daughter neurites became out of focus, whereas the mother neurite remained in focus (figure 2(C)). To directly show the growth of a neurite in 3D at high magnification, a neuronal growth cone at a neurite tip was identified and imaged for 4 h (figure 2(D); supplementary video 2). During this time period, we saw a net advancement of more than 20 $\mu$m with an average growth rate of 5.2 $\mu$m h$^{-1}$. The average advance rate of 22 growth cones in our 3D culture system was 5.6 $\pm$ 0.6 $\mu$m h$^{-1}$ ($\pm$SEM), which is similar to growth rates of bag cell neurons cultured on PLL-coated 2D glass coverslips [18]. As shown in figure 2(D), the neuronal growth cones in this 3D culture system are significantly smaller, more compact, and club-shape when compared to the large, fan-shaped growth cones developed by these neurons, when plated on PLL-coated 2D glass coverslips [11, 37, 38, 40, 44]. The average growth cone diameter in this 3D culture system is 6.4 $\pm$ 0.4 $\mu$m ($\pm$SEM; $n = 34$) compared to the large, fan-shaped growth cones in 2D that span 50–100 $\mu$m and more [11, 18]. The smaller size is likely due to the fact that the growth cones have less space to expand in the 3D gel and face an almost isotropic environment in all dimensions. In 2D culture systems, we have recently shown that smaller growth cones tend to grow faster than large fan-shaped cones [18]. Smaller, club-shaped growth cones are more commonly observed *in vivo* and in 3D cultures; thus, our findings on bag cell neurite outgrowth in 3D is consistent with previous reports [2, 46, 47]. Taken together, our novel gel mixture supports neurite regeneration of *Aplysia* bag cell neurons

in 3D, which can be readily imaged at different magnifications using our microwell device.

In addition to transmitted live cell imaging, the porous nature and optical clarity of collagen gel allows fluorescent labeling of molecules of interest after chemical fixation. To demonstrate the compatibility of our device with fluorescent imaging, we identified specific neurons with nascent neurite outgrowth 24 h after embedding (figure 3(A) inset), and fixed them 24 h later. Significant neurite outgrowth can be seen in figure 3(A), which is reminiscent of the *in vivo* morphology of mature *Aplysia* bag cell neurons [48]. The location of F-actin and microtubule cytoskeleton fits well with their known role in neurite regeneration, F-actin being concentrated in the tip of the neurite whereas microtubules being prominent along the length of the neurites (figure 3(B)). Similarly, the distribution of F-actin and microtubules in the growth cone in 3D seems to follow the same principle as in growth cones in 2D cultures [38, 49–51], with F-actin enriched in the growth cone periphery followed by microtubules in the neurite shaft (figure 3(C)). Figure 3(D) shows another example of a neuronal growth cone at higher magnification, where bundles of microtubules terminate at hotspots of F-actin. This distribution of the growth cone cytoskeleton is similar as previously reported for spiral ganglion neurons growing in 3D matrigel culture [31]. It is also consistent with earlier *in vivo* observations of pioneer growth cones in developing grasshopper embryos, which showed that microtubules follow F-actin accumulation in filopodia [52, 53], as well as with *in vitro* findings demonstrating that microtubules preferentially grow along filopodial bundles of actin filaments in the growth cone periphery [51, 54]. Because of the preservation of both morphology and antigenicity of cytoskeletal proteins after fixation in 3D, our

**Figure 3.** Cytoskeletal labeling of fixed neurons. (A) DIC image of a bag cell neuron embedded in the collagen gel showing robust neurite outgrowth at 48 h after plating. Inset shows the same cell with nascent neurites 24 h earlier at the same scale. Scale bar: 50 $\mu$m. (B) Fluorescent cytoskeletal staining of the neuron shown in A. Microtubules were stained with a primary tubulin and fluorescent secondary antibody (green), whereas F-actin was stained with Alexa-488 phalloidin (red). (C) Enlarged boxed region in B showing the localization of microtubules and F-actin along neurite and within the neuronal growth cone. Yellow indicates co-localization of microtubules and F-actin in growth cone neck. Scale bar: 12.5 $\mu$m. (D) A club-shaped neuronal growth cone at higher magnification in 3D culture system. Bundles of microtubules terminate at hotspots of F-actin. Scale bar: 5 $\mu$m.
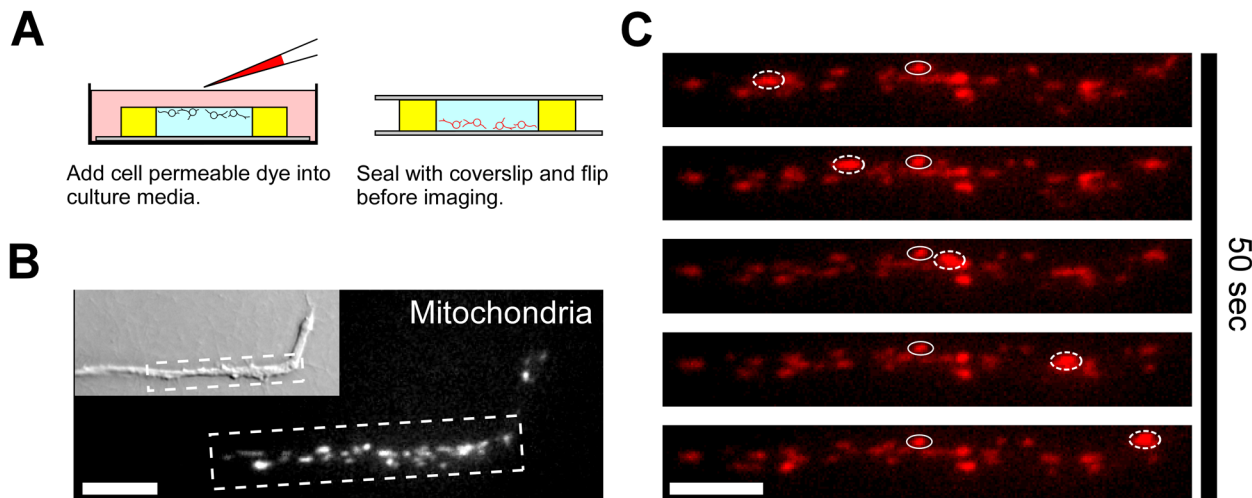


**Figure 4.** Live cell imaging of neurons in 3D using a mitochondrial dye. (A) Workflow of live cell imaging. TMRM was used to label healthy mitochondria. (B) A segment of a neurite with dense mitochondria. The neuronal growth cone is advancing towards the upper-right direction. The DIC image in the inset is shown at half the magnification. Scale bar: 10 $\mu$m. (C) Time-lapse montage of the neurite region boxed in panel B. Solid oval indicates a docked mitochondrion, whereas the dashed oval points to an anterogradely moving mitochondrion (mean rate 0.8 $\mu$m s$^{-1}$). Scale bar: 20 $\mu$m. See also supplementary video 3. A color version of this figure is available online.

microwell can serve as a reliable tool to study localization of molecules during neurite regeneration.

### 3.3. High-resolution fluorescent live cell imaging in 3D

A major benefit of our microwell is its compatibility with high-resolution live cell imaging of fluorescently labeled proteins and organelles of interest, which is in increasing demand in cell biological research. We have demonstrated this capability of our system with two live cell imaging probes as shown in figures 4 and 5. In the first approach (figure 4(A)), we added cell-permeable dye TMRM (tetramethylrhodamine methyl ester) into the cell culture media, which readily diffuses into embedded neurons and specifically labels healthy mitochondria with intact membrane potential [55]. As shown in figure 4(B), a dense population of mitochondria were successfully labeled along the neurite shaft and in the neuronal growth cone. We magnified the boxed region in
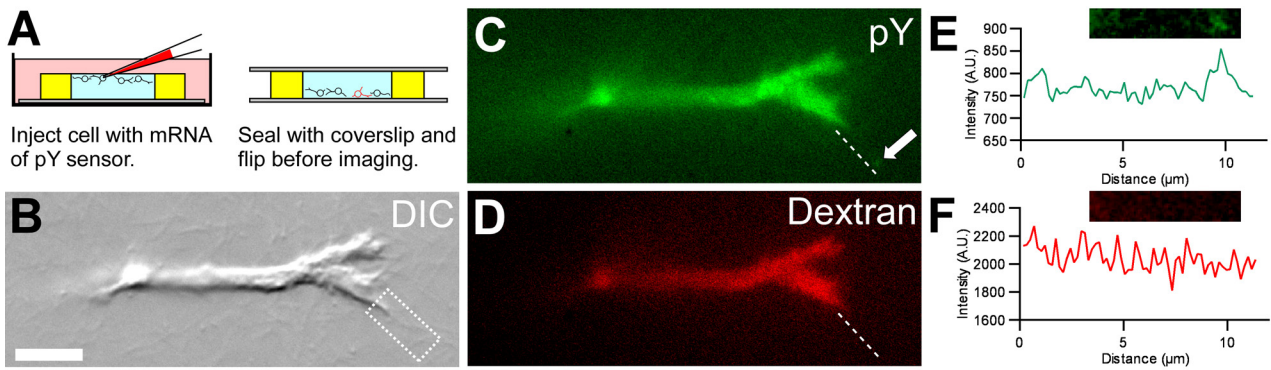
**Figure 5.** Live cell imaging of pY biosensor. (A) Workflow of live cell imaging. *In vitro* transcribed mRNA of pY biosensor was injected into the neuronal cell body together with Texas Red dextran as a volume marker. (B) DIC image of a distal neurite branching into two growth cones in 3D. Scale bar: 5 $\mu$m. (C) pY signal of the growth cone shown in B. The arrow indicates a bright spot of phosphotyrosine signal at the tip of the filopodium. (D) Texas Red dextran signal of the growth cone shown in B. No bright spot can be seen at the tip of the filopodium. (E) Fluorescent line scan of the pY signal along the filopodium next to the dotted line shown in C. The peak signal corresponds to filopodium tip. (F) Fluorescent line scan of dextran signal at the same location. No bright spot was detected at tip of the filopodium. See also supplementary video 4. A color version of this figure is available online.

figure 4(B) and assembled a time-lapse montage showing the dynamics of mitochondria in a developing neurite. Whereas the majority of mitochondria were docked during this period (the solid oval in figure 4(C) marks a stationary mitochondrion), transportation of mitochondria in both directions was evident (supplementary video 3). The average rate of anterogradely transported mitochondria is $0.5 \pm 0.1$ $\mu$m s$^{-1}$ ($\pm$SEM; $n = 5$; dashed oval in figure 4(C)), which is in good agreement with established values of fast axonal transport of mitochondria [56]. Both the high labeling efficiency and intensity as well as the transportation rate indicate the presence of active mitochondria and speak to the healthiness of regenerating neurites. Furthermore, this experiment demonstrated the feasibility of using small membrane-permeable molecules for live cell fluorescent imaging.

A second approach to introduce intracellular labeling of live cells is through ectopic expression of fluorescent proteins. In the case of embedded bag cell neurons, we can achieve this by injecting mRNA encoding fluorescent proteins into the cell bodies (figure 5(A)). This is possible because of the large soma size of *Aplysia* bag cell neurons and the short distance between neurons and gel surface. As an example, we microinjected *in vitro* transcribed mRNA of a phosphotyrosine (pY) biosensor along with Texas Red dextran as a cytosolic injection/volume marker into embedded neurons. This *Aplysia*-specific pY biosensor was adapted from a previously developed vertebrate pY biosensor [39] and contains two SH2 domains derived from *Aplysia* Src1 tyrosine kinase linked to EGFP. We initially validated this biosensor by expressing it in bag cell neurons cultured in 2D. We found a typical punctate distribution of pY signals in the growth cone including increased signal at the tips of filopodia (data not shown), which is in agreement with previous studies conducted on 2D neuronal cultures that showed enriched tyrosine phosphorylation at filopodia tips including Src-mediated phosphorylation promoting filopodia extension [40, 57–59]. Microinjection of pY biosensor mRNA into neuronal cell bodies did not prevent the regeneration of neurites in 3D (figure 5(B)). The fluorescent

signals from both ectopically expressed protein (figure 5(C)) and fluorescent injection/volume marker (figure 5(D)) could be observed in the neurite regenerating in the 3D gel. Most importantly, we found that the pY biosensor showed preferential localization to the tip of dynamic filopodia (figures 5(C) and (E); supplementary video 4) as found in 2D neuronal cultures. The pY distribution was distinct from the relative flat signal profile of fluorescent dextran along the length of filopodia (figures 5(D) and (F); supplementary video 4). In summary, these results demonstrate that we can use cell injection to express genetically encoded fluorescent proteins in neurons cultured in 3D, and perform multi-channel, high-resolution live cell imaging of regenerating neuronal growth cones.

### 3.4. Super-resolution imaging of neuronal growth cones in 3D cultures

Recent developments in sub-diffraction-limited imaging techniques have resulted in discoveries of previously hidden cellular structures such as actin rings in neuronal processes [60], and offered exciting new insights into the structural organization of macromolecular complexes especially in the cell membrane such as synapses [61–63]. To demonstrate the compatibility of our microwell device with super-resolution imaging, we immunostained microtubules and performed direct stochastic optical reconstruction microscopy (dSTORM) imaging of microtubules in distal neurites of bag cell neurons near the neuronal growth cone in 3D [64, 65]. As a contrast to the diffraction-limited image of microtubules (figure 6(A)), the reconstructed super-resolution image of the same sample revealed bundles of microtubules near the neck of the growth cone with significantly improved resolution (figure 6(B)). The axial positions of individual localized molecules within the microtubules and microtubule bundles in this example are indicated by colors and span a depth of 1 $\mu$m. Taken together, our simple microwell showed good performance when conducting super-resolution imaging of neuronal growth cones in 3D.
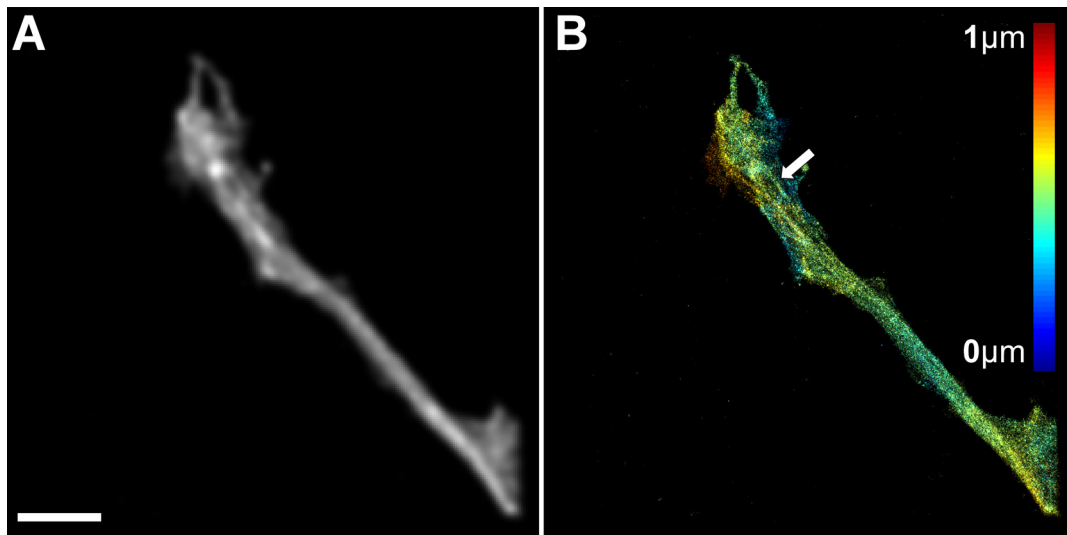
**Figure 6.** Super-resolution imaging of microtubules in distal neurite and neuronal growth cone in 3D cultures. (A) Diffraction-limited wide field fluorescent image of stained microtubules in the growth cone and distal neurite of a bag cell neuron cultured in 3D. Scale bar: 5 $\mu$m. (B) The same growth cone shown after reconstruction of 0.47 million molecules using single molecule switching nanoscopy. Arrow points to a microtubule bundle within the growth cone neck. Color encodes the axial position of labeled alpha-tubulin molecules. The growth cone was located about 5 $\mu$m from the cover glass surface.

## 4. Discussion

### 4.1. Cost-effective fabrication of a 3D neuronal cell culture device

In recent years, the supporting device for *in vitro* neurite regeneration has expanded from protein-coated glass coverslips to compliant materials, patterned substrates, and biocompatible gels [13, 16, 28, 35, 66]. This trend in creating a more physiologically relevant environment for neurons is a logical step going beyond the limitations of the traditionally used flat and rigid cell culture surfaces. However, for many laboratories such scientific reasoning is often countered by high costs of device fabrication or challenging device assembly. The motive of our work here is to build an affordable and simple microwell device to assist researchers overcome some of these barriers to 3D neuronal cell cultures. To that end, we used commonly available lab and office supplies, including standard glass coverslip, hole puncher, double-sided tape and plastic shims. The cost of our microwell is estimated to be significantly lower than most other 3D culture devices, and its assembly requires no special instrument or training. In our present study, a small amount (16 $\mu$l) of gel was sufficient to support 3D neurite outgrowth. Due to its straightforward design, we expect that individual labs will be able to easily modify microwell parameters such as size and thickness to meet their needs. In summary, the affordability and simple design of our microwell will make 3D neuronal cell culture conducive to a wider audience.

### 4.2. Proper positioning of neurons facilitates neurite outgrowth and imaging

We engineered a workflow with our microwell to optimize positioning of neurons in gel, for both sustained 3D neurite outgrowth and efficient imaging with both low- and high-power objectives. During neurite regeneration, the neuronal soma and all growing neurites interact only with collagen gel fibers and are not influenced by the gel-device interface. The uniform arrangement of neurons during embedding and the small cell-to-cell microenvironment variability increases data reproducibility and helps identifying suitable cells for imaging. We demonstrated how our microwell can be used to track neurite outgrowth from a single neuron at low magnification (figures 2(A) and 3(A)–(C); supplementary video 1), and high magnification (figures 2(B)–(D) and 3(D); supplementary video 2). Due to the proximity of the neurons to the gel surface, we were able to apply a cell permeable fluorescent dye or inject cells with mRNA for fluorescent protein expression. We performed high-resolution, live cell imaging of organelle transport along the neurite (figure 4; supplementary video 3) as well as monitoring signaling events at the growth cone (figure 5; supplementary video 4). Finally, we tested the compatibility of our 3D culture microwell with super-resolution imaging and were able to resolve bundles of microtubules in the growth cone (figure 6). All images and videos were acquired without making any modification to existing microscope platforms. Therefore, our microwell is a versatile tool for 3D neuronal cell culture, and can be adopted quickly to other cell culture systems and imaging set-ups.

### 4.3. Morphology and dynamics of Aplysia growth cones in 3D culture

We used a novel mixture of collagen to promote regeneration of *Aplysia* bag cell neurons in 3D. In comparison to outgrowth in 2D, neurites grow at similar rate but towards different directions in 3D, resulting in a growth cone morphologies that are not fan-shaped as observed in 2D cultures but more similar to growth cones observed *in vivo* in other species, such as

zebrafish [2]. At this point, it is difficult to determine the exact relative contribution of molecular versus dimensional signals to neurite growth in our gel system; however, the fact that growth cone size and advance rate could be altered by adding the gel on top of neurons cultured on PLL-coated coverslips suggests that the 3D environment supports neurite regeneration [18]. The regenerated neurites are healthy, harboring rapid transport of mitochondria along the neurite (figure 4; supplementary video 3), and display dynamic activity at the growth cone (figures 2(D) and 5; supplementary video 4). In agreement with previous studies, the basic organization of actin and microtubule cytoskeleton are consistent between 2D and 3D cultured *Aplysia* bag cell neurons (figures 3 and 6), as well as the enrichment of pY signaling at filopodia tips in the growth cone (figure 5) [38, 58]. This suggests that the central motility and signaling machinery is maintained under these different environmental conditions, which in turn result in distinct growth cone morphologies. Our system will enable future studies to further explore the exact underlying cellular and molecular mechanisms of growth cone advancement in 3D.

## 5. Conclusions

We present in this paper a low-cost and easily fabricated microwell device for *in vitro* 3D cultures of *Aplysia* bag cell neurons. To our knowledge, this is the first example of growing large *Aplysia* neurons in a defined 3D environment. We have shown that these neurons exhibit robust neurite regeneration in our novel collagen-based gel mixture. A simple procedure was developed to ensure the proper positioning of neurons in the gel to facilitate (1) sufficient neurite outgrowth in 3D, (2) efficient delivery of small molecules, (3) cell injection, and (4) high-resolution imaging. We demonstrate the utility of our microwell for various modes of high-resolution imaging of neurite outgrowth, and cytoskeletal organization, mitochondrial and pY labeling in regenerating neurites and growth cones of live neurons in 3D. Because our microwell can be conveniently assembled and used for different cell types and purposes, we believe that it could be quickly adopted by the research community for *in vitro* investigations beyond neurite regeneration of *Aplysia* neurons.

## Acknowledgments

## Conflict of interests

The authors declare no competing financial interests.

## ORCID iDs

Fang Huang https://orcid.org/0000-0003-1301-1799
Daniel M Suter https://orcid.org/0000-0002-5230-7229

## References

[1] Stoeckli E T and Landmesser L T 1995 Axonin-1, Nr-CAM, and Ng-CAM play different roles in the *in vivo* guidance of chick commissural neurons *Neuron* **14** 1165–79

[2] Hutson L D and Chien C B 2002 Pathfinding and error correction by retinal axons: the role of astray/robo2 *Neuron* **33** 205–17

[3] Chen T W *et al* 2013 Ultrasensitive fluorescent proteins for imaging neuronal activity *Nature* **499** 295–300

[4] Huisken J, Swoger J, Del Bene F, Wittbrodt J and Stelzer E H 2004 Optical sectioning deep inside live embryos by selective plane illumination microscopy *Science* **305** 1007–9

[5] Park J H, Sun W and Cui M 2015 High-resolution *in vivo* imaging of mouse brain through the intact skull *Proc. Natl Acad. Sci. USA* **112** 9236–41

[6] Chung K and Deisseroth K 2013 CLARITY for mapping the nervous system *Nat. Methods* **10** 508–13

[7] Luo X, Salgueiro Y, Beckerman S R, Lemmon V P, Tsoulfas P and Park K K 2013 Three-dimensional evaluation of retinal ganglion cell axon regeneration and pathfinding in whole mouse tissue after injury *Exp. Neurol.* **247** 653–62

[8] Byrne A B, McWhirter R D, Sekine Y, Strittmatter S M, Miller D M and Hammarlund M 2016 Inhibiting poly(ADP-ribosylation) improves axon regeneration *eLife* **5**

[9] Yogev S, Maeder C I, Cooper R, Horowitz M, Hendricks A G and Shen K 2017 Local inhibition of microtubule dynamics by dynein is required for neuronal cargo distribution *Nat. Commun.* **8** 15063

[10] Dotti C G, Sullivan C A and Banker G A 1988 The establishment of polarity by hippocampal neurons in culture *J. Neurosci.* **8** 1454–68 (http://www.jneurosci.org/content/8/4/1454.full.pdf)

[11] Hyland C, Dufresne E R and Forscher P 2014 Regeneration of Aplysia bag cell neurons is synergistically enhanced by substrate-bound hemolymph proteins and laminin *Sci. Rep.* **4** 4617

[12] Lankford K L, Waxman S G and Kocsis J D 1998 Mechanisms of enhancement of neurite regeneration *in vitro* following a conditioning sciatic nerve lesion *J. Compar. Neurol.* **391** 11–29

[13] Ahmed I, Ponery A S, Nur E K A, Kamal J, Meshel A S, Sheetz M P, Schindler M and Meiners S 2007 Morphology, cytoskeletal organization, and myosin dynamics of mouse embryonic fibroblasts cultured on nanofibrillar surfaces *Mol. Cell. Biochem.* **301** 241–9

[14] Chang S S, Guo W H, Kim Y and Wang Y L 2013 Guidance of cell migration by substrate dimension *Biophys. J.* **104** 313–21

[15] Weaver V M, Petersen O W, Wang F, Larabell C A, Briand P, Damsky C and Bissell M J 1997 Reversion of the malignant phenotype of human breast cells in three-dimensional culture and *in vivo* by integrin blocking antibodies *J. Cell Biol.* **137** 231–45

[16] Hyland C, Mertz A F, Forscher P and Dufresne E 2014 Dynamic peripheral traction forces balance stable neurite tension in regenerating Aplysia bag cell neurons *Sci. Rep.* **4** 4961

[17] Lin P W, Wu C C, Chen C H, Ho H O, Chen Y C and Sheu M T 2005 Characterization of cortical neuron outgrowth in two- and three-dimensional culture systems *J. Biomed. Mater. Res.* B **75** 146–57

[18] Ren Y and Suter D M 2016 Increase in growth cone size correlates with decrease in neurite growth rate *Neural Plast.* **2016** 3497901

[19] Li G N, Livi L L, Gourd C M, Deweerd E S and Hoffman-Kim D 2007 Genomic and morphological changes of

neuroblastoma cells in response to three-dimensional matrices *Tissue Eng.* **13** 1035–47

[20] Lee J, Cuddihy M J and Kotov N A 2008 Three-dimensional cell culture matrices: state of the art *Tissue Eng.* B **14** 61–86

[21] Desai A, Kisaalita W S, Keith C and Wu Z Z 2006 Human neuroblastoma (SH-SY5Y) cell culture and differentiation in 3D collagen hydrogels for cell-based biosensing *Biosens. Bioelectron.* **21** 1483–92

[22] Lai Y, Cheng K and Kisaalita W 2012 Three dimensional neuronal cell cultures more accurately model voltage gated calcium channel functionality in freshly dissected nerve tissue *PloS One* **7** e45074

[23] Phillips M J and Otteson D C 2011 Differential expression of neuronal genes in Muller glia in two- and three-dimensional cultures *Investigative Ophthalmol. Vis. Sci.* **52** 1439–49

[24] Breslin S and O'Driscoll L 2013 Three-dimensional cell culture: the missing link in drug discovery *Drug Discovery Today* **18** 240–9

[25] Edelman D B and Keefer E W 2005 A cultural renaissance: *in vitro* cell biology embraces three-dimensional context *Exp. Neurol.* **192** 1–6

[26] Park J W, Kim H J, Kang M W and Jeon N L 2013 Advances in microfluidics-based experimental methods for neuroscience research *Lab Chip* **13** 509–21

[27] Simi A, Amin H, Maccione A, Nieus T and Berdondini L 2014 Integration of microstructured scaffolds, neurons, and multielectrode arrays *Prog. Brain Res.* **214** 415–42

[28] Brannvall K, Bergman K, Wallenquist U, Svahn S, Bowden T, Hilborn J and Forsberg-Nilsson K 2007 Enhanced neuronal differentiation in a three-dimensional collagen-hyaluronan matrix *J. Neurosci. Res.* **85** 2138–46

[29] Ju Y E, Janmey P A, McCormick M E, Sawyer E S and Flanagan L A 2007 Enhanced neurite growth from mammalian neurons in three-dimensional salmon fibrin gels *Biomaterials* **28** 2097–108

[30] Sun G *et al* 2016 The Three-dimensional culture system with matrigel and neurotrophic factors preserves the structure and function of spiral ganglion neuron *in vitro Neural Plast.* **2016** 4280407

[31] Yan W *et al* 2017 A three-dimensional culture system with matrigel promotes purified spiral ganglion neuron survival and function *in vitro Mol. Neurobiol.* 1–15

[32] Guetta-Terrier C *et al* 2015 Protrusive waves guide 3D cell migration along nanofibers *J. Cell Biol.* **211** 683–701

[33] Lee Y S, Collins G and Arinzeh T L 2011 Neurite extension of primary neurons on electrospun piezoelectric scaffolds *Acta Biomater.* **7** 3877–86

[34] Koutsopoulos S and Zhang S 2013 Long-term three-dimensional neural tissue cultures in functionalized self-assembling peptide hydrogels, matrigel and collagen I *Acta Biomater.* **9** 5162–9

[35] Luo Y and Shoichet M S 2004 A photolabile hydrogel for guided three-dimensional cell growth and migration *Nat. Mater.* **3** 249–53

[36] Conn P J and Kaczmarek L K 1989 The bag cell neurons of Aplysia. A model for the study of the molecular mechanisms involved in the control of prolonged animal behaviors *Mol. Neurobiol.* **3** 237–73

[37] Lee A C, Decourt B and Suter D 2008 Neuronal cell cultures from aplysia for high-resolution imaging of growth cones *J. Vis. Exp.* **2008** 662

[38] Suter D M 2011 Live cell imaging of neuronal growth cone motility and guidance in vitro *Methods Mol. Biol.* **769** 65–86

[39] Kirchner J, Kam Z, Tzur G, Bershadsky A D and Geiger B 2003 Live-cell monitoring of tyrosine phosphorylation in focal adhesions following microtubule disruption *J. Sci.* **116** 975–86

[40] Wu B, Decourt B, Zabidi M A, Wuethrich L T, Kim W H, Zhou Z, MacIsaac K and Suter D M 2008 Microtubule-mediated Src tyrosine kinase trafficking in neuronal growth cones *Mol. Biol. Cell* **19** 4611–27

[41] Burke D, Patton B, Huang F, Bewersdorf J and Booth M J 2015 Adaptive optics correction of specimen-induced aberrations in single-molecule switching microscopy *Optica* **2** 177–85

[42] Huang F *et al* 2016 Ultra-high resolution 3D imaging of whole cells *Cell* **166** 1028–40

[43] Huang F *et al* 2013 Video-rate nanoscopy using sCMOS camera-specific single-molecule localization algorithms *Nat. Methods* **10** 653–8

[44] He Y, Ren Y, Wu B, Decourt B, Lee A C, Taylor A and Suter D M 2015 Src and cortactin promote lamellipodia protrusion and filopodia formation and stability in growth cones *Mol. Biol. Cell* **26** 3229–44

[45] Goodhill G J, Faville R A, Sutherland D J, Bicknell B A, Thompson A W, Pujic Z, Sun B, Kita E M and Scott E K 2015 The dynamics of growth cone morphology *BMC Biol.* **13** 10

[46] Balgude A P, Yu X, Szymanski A and Bellamkonda R V 2001 Agarose gel stiffness determines rate of DRG neurite extension in 3D cultures *Biomaterials* **22** 1077–84

[47] Graves C E, McAllister R G, Rosoff W J and Urbach J S 2009 Optical neuronal guidance in three-dimensional matrices *J. Neurosci. Methods* **179** 278–83

[48] Kaczmarek L K, Finbow M, Revel J P and Strumwasser F 1979 The morphology and coupling of Aplysia bag cells within the abdominal ganglion and in cell culture *J. Neurobiol.* **10** 535–50

[49] Bentley D and O'Connor T P 1994 Cytoskeletal events in growth cone steering *Curr. Opin. Neurobiol.* **4** 43–8

[50] Burnette D T, Schaefer A W, Ji L, Danuser G and Forscher P 2007 Filopodial actin bundles are not necessary for microtubule advance into the peripheral domain of Aplysia neuronal growth cones *Nat. Cell Biol.* **9** 1360–9

[51] Lowery L A and Van Vactor D 2009 The trip of the tip: understanding the growth cone machinery *Nat. Rev. Mol. Cell Biol.* **10** 332–43

[52] O'Connor T P and Bentley D 1993 Accumulation of actin in subsets of pioneer growth cone filopodia in response to neural and epithelial guidance cues in situ *J. Cell Biol.* **123** 935–48

[53] Sabry J H, O'Connor T P, Evans L, Toroian-Raymond A, Kirschner M and Bentley D 1991 Microtubule behavior during guidance of pioneer neuron growth cones in situ *J. Cell Biol.* **115** 381–95

[54] Schaefer A W, Kabir N and Forscher P 2002 Filopodia and actin arcs guide the assembly and transport of two populations of microtubules with unique dynamic parameters in neuronal growth cones *J. Cell Biol.* **158** 139–52

[55] Nicholls D G and Ward M W 2000 Mitochondrial membrane potential and neuronal glutamate excitotoxicity: mortality and millivolts *Trends Neurosci.* **23** 166–74

[56] Morris R L and Hollenbeck P J 1995 Axonal transport of mitochondria along microtubules and F-actin in living vertebrate neurons *J. Cell Biol.* **131** 1315–26

[57] Robles E, Woo S and Gomez T M 2005 Src-dependent tyrosine phosphorylation at the tips of growth cone filopodia promotes extension *J. Neurosci.* **25** 7669–81

[58] Suter D M and Forscher P 2001 Transmission of growth cone traction force through apCAM-cytoskeletal linkages is regulated by Src family tyrosine kinase activity *J. Cell Biol.* **155** 427–38

[59] Wu D Y, Wang L C, Mason C A and Goldberg D J 1996 Association of beta 1 integrin with phosphotyrosine in growth cone filopodia *J. Neurosci.* **16** 1470–8 (http://www.jneurosci.org/content/16/4/1470.full-text.pdf)

[60] Xu K, Zhong G and Zhuang X 2013 Actin, spectrin, and associated proteins form a periodic cytoskeletal structure in axons *Science* **339** 452–6

[61] Juette M F, Gould T J, Lessard M D, Mlodzianoski M J, Nagpure B S, Bennett B T, Hess S T and Bewersdorf J 2008 Three-dimensional sub-100 nm resolution fluorescence microscopy of thick samples *Nat. Methods* **5** 527–9

[62] Nair D, Hosy E, Petersen J D, Constals A, Giannone G, Choquet D and Sibarita J B 2013 Super-resolution imaging reveals that AMPA receptors inside synapses are dynamically organized in nanodomains regulated by PSD95 *J. Neurosci.* **33** 13204–24

[63] Owen D M, Magenau A, Williamson D and Gaus K 2012 The lipid raft hypothesis revisited—new insights on raft composition and function from super-resolution fluorescence microscopy *BioEssays* **34** 739–47

[64] Heilemann M, van de Linde S, Schuttpelz M, Kasper R, Seefeldt B, Mukherjee A, Tinnefeld P and Sauer M 2008 Subdiffraction-resolution fluorescence imaging with conventional fluorescent probes *Angew. Chem., Int. Ed. Engl.* **47** 6172–6

[65] Huang B, Jones S A, Brandenburg B and Zhuang X 2008 Whole-cell 3D STORM reveals interactions between cellular structures with nanometer-scale resolution *Nat. Methods* **5** 1047–52

[66] Georges P C, Miller W J, Meaney D F, Sawyer E S and Janmey P A 2006 Matrices with compliance comparable to that of brain tissue select neuronal over glial growth in mixed cortical cultures *Biophys. J.* **90** 3012–8